Mechanics of Materials 17 (1994) 135–145
Elsevier

On the strain and strain rate dependence of the fraction of plastic work converted to heat: an experimental study using high speed infrared detectors and the Kolsky bar [1]

J.J. Mason, A.J. Rosakis and G. Ravichandran

California Institute of Technology, 105-50, Pasadena, CA 911252, USA

Received 6 November 1992; revised version received 25 March 1993

This paper is dedicated to the memory of Professors J. Duffy and H. Kolsky of Brown University, and the work presented here is based on pioneering experimental techniques developed by them.

The conversion of plastic work to heat at high strain rates gives rise to a significant temperature increase which contributes to thermal softening in the constitutive response of many materials. This investigation systematically examines the rate of conversion of plastic work to heat in metals using a Kolsky (split Hopkinson) pressure bar and a high-speed infrared detector array. Several experiments are performed, and the work rate to heat rate conversion fraction, the relative rate at which plastic work is converted to heat, is reported for 4340 steel, 2024 aluminum and Ti–6Al–4V titanium alloys undergoing high strain and high strain rate deformation. The functional dependence of this quantity upon strain and strain rate is also reported for these metals. This quantity represents the strength of the coupling term between temperature and mechanical fields in thermomechanical problems involving plastic flow. The experimental measurement of this constitutive function is important since it is an integral part of the formulation of coupled thermomechanical field equations, and it plays an important role in failure mode selection – such as the formation of adiabatic shear bands – in metals deforming at high strain rates.

1. Introduction

In coupled thermomechanical problems an additional field equation is added to the usual field equations. This additional equation, the heat conduction equation, provides a link between mechanical deformation fields and an additional unknown, the temperature field, $T(\boldsymbol{x}, t)$, and is given by

$$\alpha \nabla^2 T - \dot{T} = -\frac{\beta \boldsymbol{\sigma} \cdot \dot{\boldsymbol{\epsilon}}^{\mathrm{p}}}{\rho c_p} + \frac{\kappa}{\rho c_p} \frac{E}{(1-2\nu)} T_0 \operatorname{tr}(\dot{\boldsymbol{\epsilon}}^{\mathrm{e}}), \quad (1)$$

where the dot refers to differentiation with respect to time, α is the thermal diffusivity, ρ is the density, c_p is the heat capacity, β is defined below, $\boldsymbol{\sigma}$ is the stress, $\dot{\boldsymbol{\epsilon}}^{\mathrm{p}}$ is the plastic strain rate, κ is the coefficient of thermal expansion, E is Young's modulus, ν is Poisson's ratio, $\dot{\boldsymbol{\epsilon}}^{\mathrm{e}}$ is the elastic strain rate and T_0 is the initial or ambient temperature. The first term on the right represents heating due to irreversible plastic deformation (Taylor and Quinney, 1934; Bever et al., 1973) and the second term represents heating due to the reversible thermoelastic effect (Sneddon and Berry, 1958). If elasticity is neglected and adiabatic conditions prevail, then the heat conduction equation takes a more simple form, i.e.;

$$\rho c_p \dot{T} = \beta \boldsymbol{\sigma} \cdot \dot{\boldsymbol{\epsilon}}^{\mathrm{p}} = \beta \dot{W}^{\mathrm{p}}, \quad (2)$$

[1] The research of A.J. Rosakis and J.J. Mason is performed with support from the Office of Naval Research under grant N00014-90-J-1340, and the research of G. Ravichandran is performed with support from the National Science Foundation under a Presidential Young Investigator award.

SSDI 0167-6636(93)E0069-E

where

$$\beta = \frac{\rho c_p \dot{T}}{\dot{W}^{\mathrm{p}}}. \tag{3}$$

Obviously, even for these simple conditions it is necessary to know the material parameters such as β, the work rate to heat rate conversion fraction, and c_p, the heat capacity which may depend upon temperature, before useful solutions to thermomechanics problems can be obtained.

Although c_p may be found in tables (sometimes as a function of temperature), β is not commonly available. Often β is simply assumed to be a constant in the range 0.85–1.00; a practice that dates back to the work of Taylor and Quinney (1934). They determined β using calorimetric methods to measure the heat produced during quasi-static deformation. The remaining work is usually attributed to the stored strain energy e.g. dislocations, defects and their interactions. However, it is known that β may depend upon strain. Many investigations (Bever et al., 1973) in the past have been concerned with a quantity related to β, the fraction of stored energy being defined as

$$f = 1 - \frac{\rho c_p T}{W^{\mathrm{p}}}. \tag{4}$$

They have reported that this material property depends upon strain. Since β may be expressed in terms of f, it is clear that β will depend upon strain as well. At least two models have been proposed for predicting the dependence of β or f upon strain, representing two mechanisms for the storage of energy in a material. In the first model, dislocation density is assumed to increase with strain at a rate that is proportional to the slope of the stress–strain curve. The energy per unit of dislocation density is estimated, and the relative rate at which work is converted to heat may then be related to the work hardening exponent (Bever et al., 1973; Zehnder, 1991). In the second model, the stored macroscopic strain energy is calculated for a polycrystalline solid made up of elastic–perfectly-plastic crystals, and the stored energy is related to the reciprocal of plastic work, $\int \epsilon^{\mathrm{p}}\, \mathrm{d}\sigma$ (Aravas et al., 1990). The two models

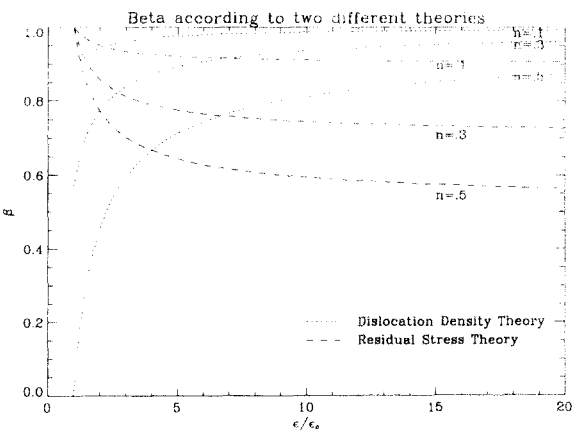

Fig. 1. Theoretical prediction of the dependence of β, the work rate to heat rate conversion fraction, upon strain and hardening exponent, n, in metals. (For the model of Zehnder $A = 1$.)

produce different predictions for the dependence of β upon strain. For a power law hardening material,

$$\sigma = \begin{cases} \sigma_0(\epsilon/\epsilon_0), & \text{for } \sigma \leqslant \sigma_0, \\ \sigma_0(\epsilon/\epsilon_0)^n, & \text{for } \sigma \geqslant \sigma_0, \end{cases} \tag{5}$$

the two separate models predict

$$\beta(|\epsilon|) = \begin{cases} \dfrac{(\epsilon/\epsilon_0)^{1-n} - 2An}{(\epsilon/\epsilon_0)^{1-n} - n}, \\ \text{for dislocation theory,} \\ \dfrac{(1-n)(\epsilon/\epsilon_0)^n}{(\epsilon/\epsilon_0)^n - n(\epsilon/\epsilon_0)^{2n-1}}, \\ \text{for strain energy theory,} \end{cases} \tag{6}$$

where σ_0 and ϵ_0 are the yield stress and strain for the material, respectively, and n is the hardening exponent. The results may be seen in Fig. 1 for different values of the hardening exponent, n. In the dislocation based model, β increases with strain while in the strain energy based model the opposite is true. (The models have been adapted to produce a prediction for β rather than f when necessary.) As evident from Eq. (6), the dislocation theory contains an unknown parameter, A, that essentially assumes the role of a fitting parameter. The residual stress theory is exact for a

material made up of elastic–perfectly-plastic crystals, but it only serves as a lower bound on β for work hardening crystals. Comparison of these models with experiments on copper at low strain rates (Williams, 1965) showed the model of Zehnder (1991) to be more accurate for that material.

Little is known about the dependence of β upon strain rate. Some early work has shown that the stored energy in drawn wires has a maximum when plotted with respect to drawing rate (Bever et al., 1973). This maximum is attributed to the thermal annihilation of dislocations at higher drawing rates resulting in a decrease in stored energy. Also, if one uses the above theories for strain dependence of β for all strain rates, then the materials exhibiting strain rate dependence in their mechanical behavior should also exhibit strain rate dependence in β. For example, copper is weakly strain rate dependent for strain rates in the range 10^{-4}–10^{3}, and, consequently, it has shown a very small strain rate dependence in the work rate to heat rate conversion fraction, β (Williams, 1965). Even though the work rate to heat rate conversion fraction, β, shows some indication of being a material dependent function of both strain and strain rate i.e. $\beta = \beta(|\epsilon|, |\dot{\epsilon}|)$, virtually no work has systematically tried to investigate the dependence of β upon strain rate for many structural materials. The experimental procedure introduced here provides, for the first time, a simple means by which to carry out such investigations.

It is important to investigate the behavior of β under a variety of deformation histories because of its role in thermomechanics. In dynamic plasticity experiments the conversion of plastic work to heat can lead to thermal softening and instabilities in the deformation (for example see Clifton et al., 1984; Batra and Wright, 1988). Any numerical modelling of dynamic plastic deformation that includes the effects of heat generation would require complete knowledge of the behavior of the material constitutive functions, including β, during all phases of deformation before accurate modeling of any unstable behavior such as adiabatic shear band formation (Duffy, 1984; Giovanola, 1988) may be achieved. Motivated by the above concerns our goal here is to report on the initial steps of a study whose aim is to investigate the functional dependence of β on $|\epsilon|$ and $|\dot{\epsilon}|$ for a variety of loading regimes.

2. Experimental apparatus

The Kolsky pressure bar is used to deform the materials at high strain rates (≈ 1000–$3000\ s^{-1}$) in this investigation. The incident, $\epsilon_I(t)$, reflected, $\epsilon_R(t)$, and transmitted, $\epsilon_T(t)$, strain signals are recorded by strain gauges attached to the input and output bars. The stress, strain rate, strain and average velocity of the deforming specimen can be determined from the recorded incident, reflected and transmitted pulses assuming that the specimen deforms *homogeneously* (Kolsky, 1949):

$$\begin{aligned}
\sigma(t) &= E_{\text{bar}} \frac{A_0}{A} \epsilon_T(t), \\
\dot{\epsilon}(t) &= -\frac{2c_0}{L} \epsilon_R(t), \\
\epsilon(t) &= \int_0^t \dot{\epsilon}(\tau)\, d\tau, \\
\bar{v}(t) &= \frac{2c_0}{L} \epsilon_I(t),
\end{aligned} \tag{7}$$

where E_{bar} is Young's modulus of the bar, A_0 and A are the cross sectional area of the bar and the specimen, respectively, c_0 is the one dimensional wave speed in the bar, L is the specimen length and $\bar{v}$ is the average specimen velocity. Note that the average velocity is nonzero, meaning that the specimen translates past a stationary observer. For further details of the pressure bar technique the reader is referred to Lindholm (1964) and Follansbee (1985).

In order to record the temperature rise in the Kolsky pressure bar experiments a stationary, focused, high-speed, infrared detector array is used. For details regarding the detector array time response and characteristics see Zehnder and Rosakis (1991, 1993). The array is shown in Fig. 2. The detectors are calibrated by heating a sample – with controlled surface finish – of the specimen material to a known temperature while

simultaneously recording the detector output voltage. The calibration procedure precludes the need for any knowledge of the specimen emissivity and, thus, greatly simplifies the temperature measurement procedure. A sample calibration curve corresponding to a 4340 specimen may be seen in Fig. 3. Although they are not shown, calibration curves are evaluated for every material investigated here. In each case the resulting curve is qualitatively very similar to Fig. 3. The dependence of the calibration curve upon surface finish is investigated since the specimen surface finish may change during deformation in the Kolsky bar. Two roughnesses were chosen; one representing the specimen before deformation, 600 grit finish, and one representing the specimen after deformation, 120 grit finish. Minimal dependence upon surface finish is seen. For the two very different surface finishes the calibration is very nearly the same and within the scatter of either calibration curve. This is largely due to the longer wavelength of infrared radiation and the

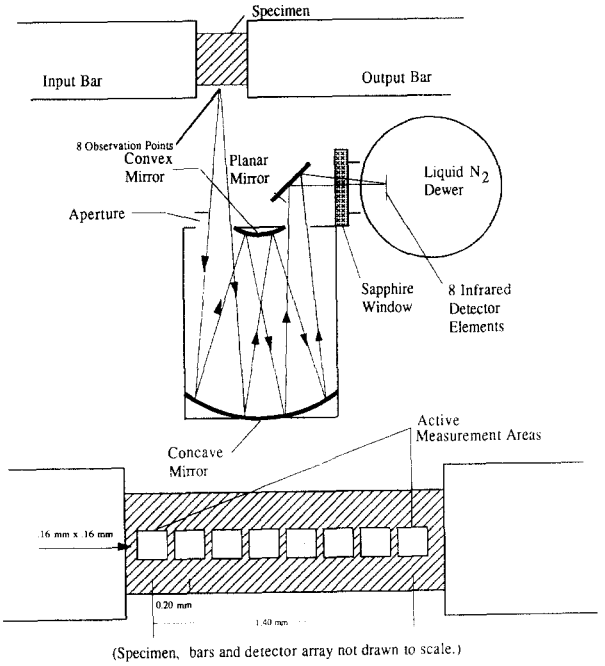

Fig. 2. A schematic representation of the high speed I-R detector array focussed on a specimen in a Kolsky pressure bar. The detector array size and orientation as focussed on the specimen is also shown.

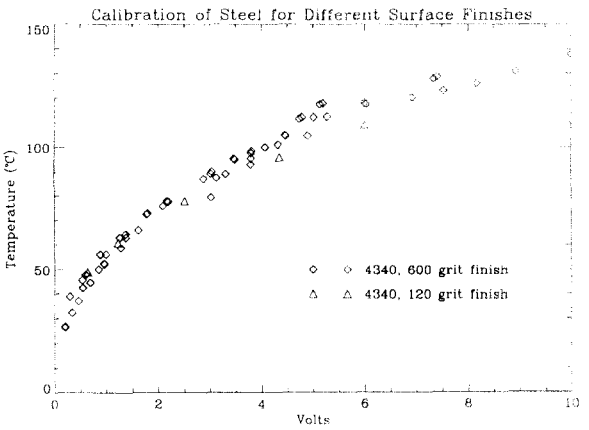

Fig. 3. Calibration of the I-R detectors. The dependence of the calibration curve upon surface finish is shown to be minimal.

detector characteristics. (The detectors integrate energy over a band of infrared wavelengths.) Some materials exhibit a stronger dependence upon surface finish than others; colored metals such as brass and copper are somewhat more sensitive to finish. Regardless, it suffices to say that for the metals studied here, the effects of change in surface finish during deformation are negligible. Further details of the high speed infrared measurement technique can be found in Duffy (1984) and in Zehnder and Rosakis (1991, 1993).

Assuming that homogeneous deformation of the specimen occurs, one may easily calculate the plastic work rate density from the Kolsky bar using relations (7) and

$$\dot{W}^{\mathrm{P}} = \boldsymbol{\sigma} \cdot \dot{\boldsymbol{\epsilon}}^{\mathrm{P}}. \tag{8}$$

By measuring the temperature and differentiating it with respect to time, $\dot{T}(t)$ is estimated, and by assuming that adiabatic conditions apply during the experiment, β is calculated from Eq. (3). The density and heat capacity (with its dependence upon temperature) may be found in the literature (e.g., *Aerospace Structural Materials Handbook*, 1985) for the materials investigated; 4340 steel, Ti–6Al–4V and 2024 Al. Fortunately, it is seen that the heat capacity for each of these materials does not change significantly over the range of material temperatures anticipated during the experiments (20–130°C).

3. Results and discussion

Typical results of the experiments are shown for 2024 aluminum in Fig. 4. The figure shows the time history of strain of the input and output bars as well as the time history of the voltage output of two detectors focussed on the specimen surface at two points 1.4 mm apart. It should be noted that the temperature reaches its maximum value within 150 μs during loading and remains constant once unloading occurs; thus, the process is adiabatic. As expected from a simple model of heat conduction in the Kolsky bar (Mason, 1993), adiabatic conditions were observed for all materials studied here. Also, the two detector output voltages nearly coincide during loading of the specimen. Since the process is adiabatic, Eq. (2) holds, and, since the temperature is nearly independent of position, Eq. (2) indicates that the plastic work rate is also nearly independent of position. Thus, the deformation is homogeneous. It is also worth observing that there is a second temperature rise in the specimen due to the reflection of waves from the free end of the input bar which results in a second loading of the specimen. In softer materials such as 2024 aluminum this secondary temperature rise is significant. Lastly, it is observed that the output of one of the detectors drops shortly after the second loading of the specimen by the reflected wave begins. This is because the specimen and input bar are moving. The input bar has moved in front of one detector causing a lower temperature to be measured there.

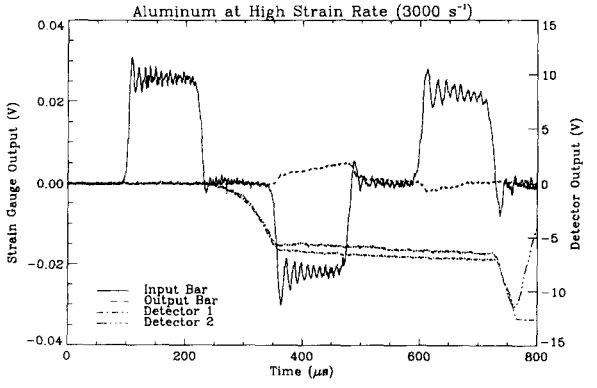

Fig. 4. The results of a typical split Hopkinson bar experiment on 2024 aluminum. The transmitted and reflected signals are delayed with respect to the temperature signal because the strain gauge measurements are made at a finite distance from the specimen.

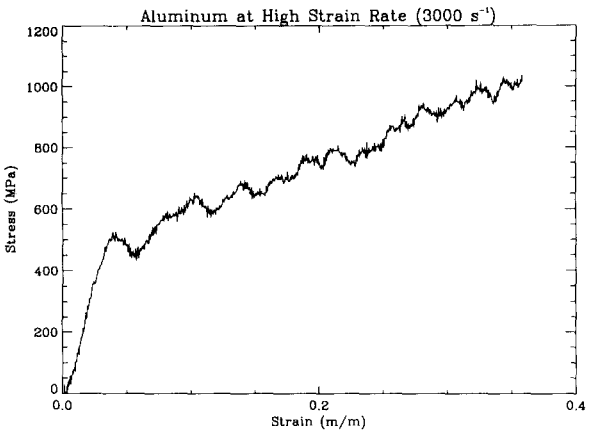

Fig. 5. The stress–strain relationship for 2024 aluminum at high strain rate (3000 s^{-1}). The hardening exponent from a fit of the power law constitutive equation, Eq. (5), is calculated to be 0.31.

The stress–strain curve for 2024 aluminum calculated from the Kolsky bar equations is shown in Fig. 5. Note that three dimensional effects and lack of equilibrium in the specimen at short times in the Kolsky bar result in inaccuracies at low strains (Follansbee and Frantz, 1983) and that the elastic behavior of the specimen is not captured. These effects add to the uncertainty in the calculation of β at low strains ($\epsilon \leqslant 3\%$). The hardening exponent for 2024 Al is 0.31 when the constitutive model in Eq. (5) is fitted to the experimental results. The plastic work rate may be calculated using Eqs. (7) and (8) and is shown in Fig. 6. An approximation of the plastic work by a linear fit of the experimental data with respect to time is also shown in the figure. This approximation is considered a valid estimate of the true plastic work rate since the oscillations in the experimentally observed plastic work rate are due to three dimensional wave propagation in the input and output bars of the apparatus. In the calculations of β presented here the fitted approximation is used.

The temperature measurement also suffers from inaccuracies at low temperatures because of inherent noise in the signal and the slope of the calibration curve. At low voltages the calibration curve slope becomes very large, therefore a small amount in noise can result in large fluctuation in temperature. This makes the calculation of β uncertain for low strains ($\rho \leqslant 3\%$) where temperature rise is still small (below 10°C).

The most significant difficulty in calculating β however is due to the problems associated with differentiation of the measured temperature. Differentiation of a noisy signal has inherent instabilities, and usual numerical differentiation schemes such as the central difference method (Beyer, 1987) do not work because they are formulated for numerically exact functions. The noise in the function to be differentiated by such methods must be much smaller than the sampling time. That is not the case here, and an alternate method is necessary to accurately differentiate the temperature rise. It is not sufficient to simply fit a known function to the temperature measurement in this case because the exact form of the expected result is not known and two equally good fits can result in dramatically different derivatives. Consequently, the method of Vasin (1973) and Groetsch (1992) is used to differentiate the temperature measurement. In this method

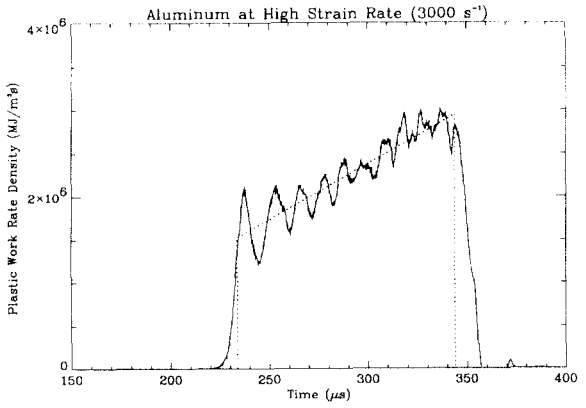

Fig. 6. The plastic work rate density as calculated using Eqs. (7) and (8). The oscillations are due to three-dimensional wave propagation in the bar. A linear fit to the data shown as a dotted line is used in calculations of β in Fig. 8.

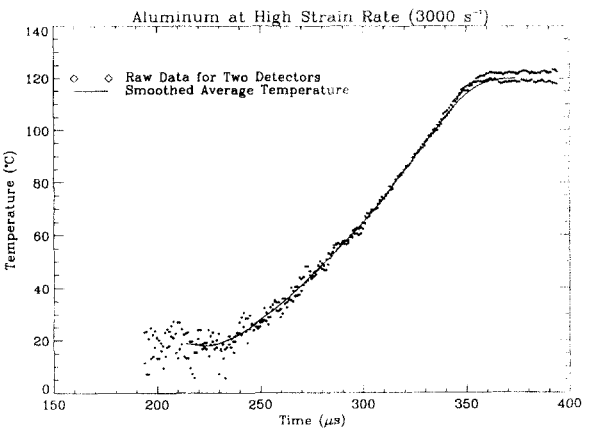

Fig. 7. The temperature data for 2024 aluminum. The solid line represents the smoothed function which is differentiated using the method of Vasin (1973), and Groetsch (1992).

a weighted average smoothing function is used to differentiate a noisy signal, $g(t)$ i.e.

$$\omega_{t_0}(t) = \begin{cases} \dfrac{0.825}{t_0}\exp\left[t^2/\left(t^2 - t_0^2\right)\right], \\ \quad \text{for } |t| < t_0, \\ 0, \quad \text{for } |t| \geqslant t_0, \end{cases} \tag{9}$$

where

$$g_s(t) = \int_{t-t_0}^{t+t_0} \omega_{t_0}(t-s)g(s)\,\mathrm{d}s$$

$$= \omega_{t_0} g, \tag{10}$$

where t_0 is the half width of the time over which a weighted average of the noisy signal is taken and $g_s(t)$ is the smoothed function. An example of the smoothed temperature signal with $t_0 = 20$ μs may be seen in Fig. 7 plotted with both noisy signals. Further precautions were taken by averaging the two temperature signals before smoothing to reduce some of the noise at low temperature. Differentiation of the noisy signal, $g(t)$, is carried out by using the relationship

$$g_s'(t) = \omega_{t_0}' g (= \omega_{t_0} g'). \tag{11}$$

Consequently, the derivative is actually found by differentiating the smoothing function, $\omega_{t_0}(t)$, and

integrating the convolution in Eq. (11) for all points of the temperature signal. Multiplying the derivative of temperature by ρc_p and using Eq. (3) results in the evaluation of β.

The dependence of the work rate to heat rate conversion fraction, β, upon strain for a nominal strain rate of 3000 s^{-1} and corresponding to the raw data shown in Figs. 4–7 is plotted in Fig. 8. It can be seen that β for 2024 aluminum is strongly strain dependent; initially the relative rate at which work is converted to heat is approximately 0.5 rising with strain to the traditionally accepted 0.85–1.00 range for metals (Taylor and Quinney, 1934; Bever et al., 1973). The trend qualitatively follows the model of Zehnder (1991) and not that of Aravas et al. (1990). Since the model of Zehnder is known to be more accurate than the model of Aravas et al. for strain rate insensitive copper at low strain rates and nominally high strain rates (10^3 s^{-1}) and since quasi-static testing of the 2024 aluminum by the authors shows that the stress–strain curve has only a weak strain rate dependence over the same strain rate range, it is concluded that β for 2024 aluminum at high strain rates behaves much the same as it would be expected to behave at low strain rates. This is also supported by the finding that the large strain value calculated for β at high strain rates, 0.85, corresponds well with general observations of β

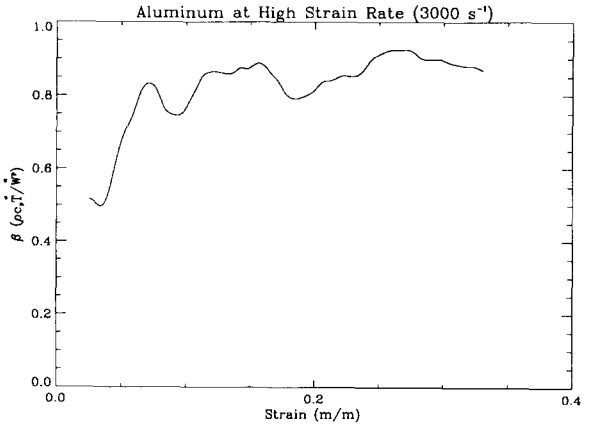

Fig. 8. The work rate to heat rate conversion fraction for 2024 aluminum. Good qualitative agreement is seen between the experimental results shown here and the theoretical prediction of Zehnder in Fig. 1.

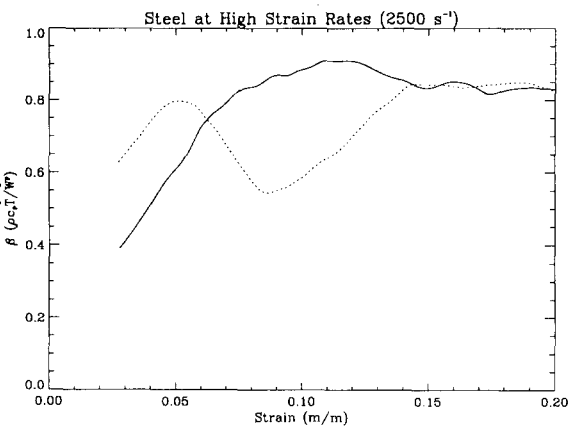

Fig. 9. The work rate to heat rate conversion fraction for steel. The calculation of β has been carried out for each detector individually. The anomalous result in one detector at lower strains is due to inhomogeneous deformation of the steel.

made for all metals at low strain rates. Thus, strain rate dependence in β is not found in 2024 aluminum for strain rates up to $\dot{\epsilon} \approx 3000$ s^{-1}.

In Fig. 9 the same calculation has been carried out for 4340 steel. Here the signals from each detector were treated individually to show some unexpected behavior. It can be seen that for one detector in early parts of the experiment the value of β varies noticeably. However, on the other detector the value of β is a smoothly increasing function of strain and in qualitative agreement with the results for 2024 aluminum. The final value of β for both detectors, 0.85, is in agreement with earlier preliminary experiments on 4340 steel (Rosakis et al., 1992). The disagreement between two detectors in the calculation of β is due to inhomogeneous deformations. In Fig. 10 it can be seen that temperature spikes can occur on one detector during the initial deformation of 4340 steel. These spikes are never observed in 2024 aluminum or Ti–6Al–4V titanium, but they occur regularly, although not consistently, in experiments with 4340 steel. Because adiabatic conditions prevail, a spike in the temperature measurement indicates that an inhomogeneity, perhaps similar to the formation of Luder's bands, has formed in the early stages of the deformation of 4340 steel. The spike disap-

pears because the specimen is moving and the inhomogeneity translates away from the focussed detector. Notice that the other detector also shows some transient temperature rise due to the inhomogeneity. The formation of such inhomogeneities violates the assumptions of the Kolsky bar equations, Eq. (7). Consequently, the plastic work reported for that portion of the experiment is only an *average* value and does not reflect the local value of the plastic work rate density near the inhomogeneity. At later times it is likely that the specimen is deforming more homogeneously, and, consequently, the results are more repeatable. Following the arguments used for 2024 aluminum it is concluded that strong strain dependence but no strain rate dependence of β is observed in 4340 steel up to strain rates of 3000 s^{-1}.

The experiments on Ti–6Al–4V titanium indicate that it also suffered from inhomogeneous deformations. This material, however, deformed in a different fashion than the steel. The Ti–6Al–4V titanium did not show large initial spikes in the temperature measurement. Rather, it deformed inhomogeneously over a larger scale, resulting in two slightly different temperature measurements for each detector over the duration of the loading. In Fig. 11 it can be seen that the detector measurements differ not more than 10%

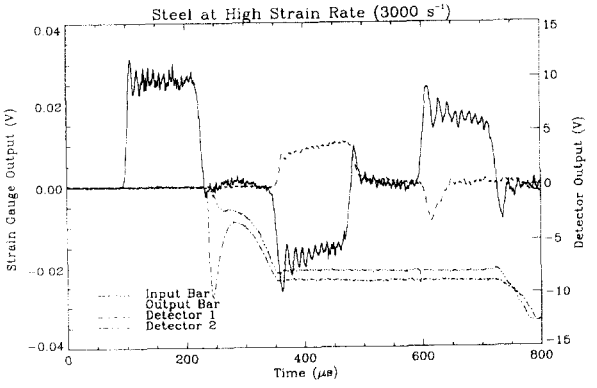

Fig. 10. The raw data for an experiment using 4340 steel. These results show a spike in one of the two temperature detectors due to a localized deformation. Such spikes are not always repeatedly observed in steel although they are never observed in Ti–6Al–4V titanium or 2024 aluminum.

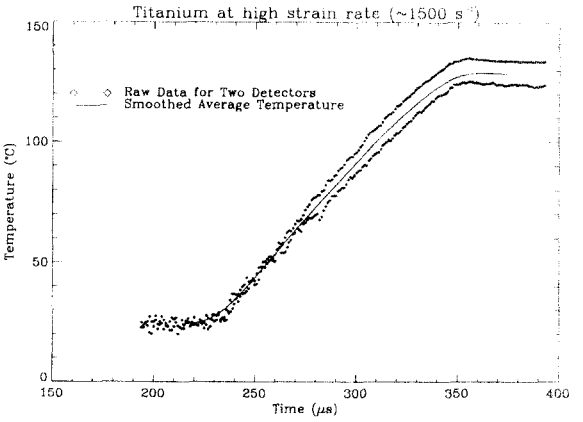

Fig. 11. The temperatures measured by each of two detectors during an experiment of Ti–6Al–4V titanium are slightly different. This is due to inhomogeneous deformation over a scale that is larger than the separation of the detectors. The shape of the curve i.e. a decreasing slope, however, is invariant with respect to measurement location.

over the full length of the experiment. However, the shape and curvature of these curves remain equivalent. It was observed that the final temperature measured varies slightly with the initial placement of the detectors along the axial coordinate of the specimen, but the shape and curvature do not vary with measurement location. Therefore, the deformation varies over more than the separation of the two detectors (1.4 mm). Since the Kolsky bar reports an *average* measure of the plastic work rate for inhomogeneously deforming materials, an *average* of the two temperature measurements is used to calculate the work rate to heat rate conversion fraction, β. The result is shown in Fig. 12. Note that the form of β for Ti–6Al–4V titanium is different than that of 2024 aluminum and that it is in better agreement with the model of Zehnder (1990) at low strains (up to 5%). At higher strains the same curve is in better qualitative agreement with the model of Aravas et al. (1990). Since quasi-static measurement of the stress–strain behavior of Ti–6Al–4V titanium by the authors shows this alloy to be strain rate sensitive, this difference between the behavior of Ti–6Al–4V and the behavior of 4340 steel or 2024 aluminum – in the same strain rate range – may be connected to the strain rate

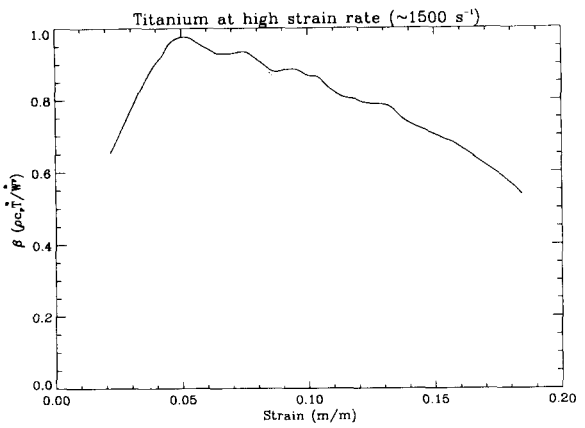

Fig. 12. The work rate to heat rate conversion fraction is calculated for Ti–6Al–4V titanium using the average of the temperature of the two detectors. It is seen that the form of the result qualitatively follows the prediction of Zehnder (1991) at low strains and the prediction of Aravas et al. (1990) at high strains. (See Fig. 1.)

sensitivity of the Ti–6Al–4V titanium. At higher strain rates twinning becomes a significant deformation mechanism in Ti–6Al–4V (Follansbee and Gray, 1989) resulting in a higher percentage of plastic work being stored in the material rather than converted to heat. Further work at lower strain rates as well as at high strain rates using the full detector array combined with post-mortem examination of the specimens should shed more light on this issue.

4. Conclusions

This work describes the first attempt to quantify the functional dependence of the plastic work rate to heat rate conversion fraction, β, on strain and strain rate in a range of metals. The main conclusions can be summarized as follows:

(1) Adiabatic conditions exist in the Kolsky bar for experiments on 4340 steel, 2024 aluminum and Ti–6Al–4V titanium when experimental times were shorter than 800 μs. This fact greatly simplifies the thermomechanical analysis of specimen deformation in the Kolsky bar.

(2) It is possible to measure the dependence of β upon strain and strain rate using the Kolsky bar and high speed temperature detectors provided the specimen deforms uniformly or nearly uniformly.

(3) For nominally strain rate independent solids, the dependence of β upon strain at high strain rate (1000–3000 s^{-1}) roughly follows the dependence expected at low strain rates. The model of Zehnder (1991) produces an acceptable qualitative prediction of this dependence. Consequently, significant strain rate dependence of β for 2024 Al and 4340 steel is not detected over a large range of strain rates (10^{-3} to 10^{3} s^{-1}). However, this is to be expected since neither materials showed strain rate dependence in their mechanical properties.

(4) Strain rate sensitive Ti–6Al–4V titanium exhibited interesting behavior at high strain rates. The measured dependence of β upon strain for this material did not follow the qualitative trends observed in strain rate insensitive 2024 aluminum and 4340 steel. The model of Zehnder (1991) qualitatively described β at low strains while the model of Aravas et al. (1990) gave a better qualitative description at high strains. This difference may be connected to the strain rate sensitivity of the material. Further investigation is required.

(5) The reflection of input stress waves from the free end of the input bar of the Kolsky bar lead to significant temperature rises in the specimen subsequent to the conclusion of the initial, recorded loading. This fact must be considered if post-mortem examination of the specimens is to be performed since the microstructure of the material may be influenced by the high temperatures generated during repeated loading. Repeated loading can be eliminated using the stress reversal Kolsky bar set up (Nemat-Nasser et al., 1991).

These results have significant implications in the study of the conditions preceding and governing adiabatic shear band formation and shear band growth as well as on the establishment of a criterion governing dynamic failure mode selection in rate sensitive materials. This is because the work rate to heat rate conversion fraction, β, serves as a measure of the strength of the coupling term, in Eq. (1), between the temperature and mechanical fields. The temperature rise gov-

erned by Eq. (1) can be significant leading to thermal softening and to subsequent shear localization in many materials. When modelling thermomechanical behavior of materials β is usually assumed to be a constant. For example, in thermomechanical models of shear band formation (Clifton et al., 1984; Belytschko et al., 1991; Wright and Ockendon, 1992), in thermomechanical finite element simulations of dynamic failure mode transitions (Lee, 1990) and in general thermomechanical computational codes (Simo and Miehe, 1992), β is assumed to be a constant in the traditionally accepted range of 0.85–1.00. However, as shown here, this assumption may not be correct for all metals, and serious consideration of the variation of β with strain and strain rate may be necessary to properly account for the strength of the thermomechanical coupling and to accurately model material behavior. For example, β in Ti–6Al–4V deformed at high strain rates is significantly dependent upon strain, and, for strains higher than 5%, β decreases from 1 to 0.5 (at 20%, see Fig. 12). This decreasing trend may continue for strains beyond 20%. Also, this strong variation of β with strain may suggest that β is dependent upon strain rate as well. Such strain and strain rate sensitivity in the mechanism of converting plastic work to heat for this material may play an important role in the determination of the width of shear localization zones, in the determination of the maximum temperature in such zones and, ultimately, in the determination of a critical shear localization or failure mode selection criterion.

References

Aravas, N., K-S. Kim and F.A. Leckie (1990), On the calculations of the stored energy of cold work, *J. Eng. Mater. Technol. 112*, 465.

Aerospace Structural Materials Handbook (1989), Metals and Ceramics Information Center, Battelle Columbus Laboratories, Columbus, OH.

Batra, R.C. and T.W. Wright (1988), A comparison of solutions for adiabatic shear banding by forward-difference and Crank–Nicolson methods, *Commun. Appl. Numer. Meth. 4*, 741.

Bever, M.B., D.L. Holt and A.L. Titchener (1973), The stored energy of cold work, *Progr. Mater. Sci. 17*, 1.

Beyer, W.H. (1987), *CRC Standard Mathematical Tables*, 28th Ed., CRC Press, Inc., Boca Raton, Florida, p. 449.

Belytschko, T., B. Moran and M. Kulkarni (1991), On the crucial role of imperfections in quasi-static viscoplastic solutions, *J. Appl. Mech. 58*, 658.

Clifton, R.J., J. Duffy, K.A. Hartley and T.J. Shawki (1984), On critical conditions for shear band formation at high strain rates, *Scr. Met. 18*, 443.

Duffy, J., (1984), Temperature measurements during the deformation of shear bands in a structural steel, in: G.J. Dvorak and R.T. Shield, eds., *Mechanics of Material Behavior*, Elsevier, Amsterdam, p. 75.

Follansbee, P.S. (1985), The split Hopkinson bar, *Metals Handbook*, 9th Ed., American Society for Metals, Metals Park, OH, Vol. 8, 198.

Follansbee, P.S. and C. Frantz (1983), Wave propagation in the split Hopkinson pressure bar, *J. Eng. Mater. Technol. 105*, 61.

Follansbee, P.S. and G.T. Gray (1989), An analysis of the low temperature low and high strain-rate deformation of Ti–6Al–4V, *Metall. Trans. A 20A*, 863.

Giovanola, J.H. (1988), Adiabatic shear banding under pure shear loading, Part I: Direct observation of strain localization and energy dissipation measurements, *Mech. Mater. 7*, 59.

Groetsch, C.W. (1992), Optimal order of accuracy in Vasin's method for differentiation of noisy functions, *J. Optimization Theory Appl. 74*, 373.

Kolsky, H. (1949), An investigation of the mechanical properties of materials at very high rates of loading, *Proc. R. Soc. B62*, 676.

Lee, Y.J. (1990), Problems associated with dynamic fracture under high strain rate loading, Ph.D. Thesis, Division of Engineering, Brown University.

Lindholm, U.S. (1964), Some experiments with the Split Hopkinson Pressure Bar, *J. Mech. Phys. Solids 12*, 317.

Mason, J.J. (1993), The mechanisms and effects of heat generation at the tip of a dynamic crack, Ph.D. Thesis, Graduate Aeronautical Laboratories, California Institute of Technology, Pasadena, CA, 91125.

Nemat-Nasser, S., J.B. Isaacs and J.E. Starret (1991), Hopkinson techniques for dynamic recovery experiments, *Proc. R. Soc. London. A435*, 371.

Rosakis, A.J., J.J. Mason and G. Ravichandran (1992), The conversion of plastic work to heat around a dynamically propagating crack in metals, *J. Mech. Behavior Mater. 4(4)*, 375.

Simo, J.C. and C. Miehe (1992), Associative coupled thermoplasticity at finite strains formulation, numerical analysis and implementation, *Comput. Meth. 98*, 41.

Sneddon, I.N. and D.S. Berry (1958), The classical theory of elasticity, in: S. Flugge, ed., *Handbuch der Physik*, Vol. VI, Springer, Berlin, p. 123.

Taylor, G.I. and M.A. Quinney (1934), The latent energy remaining in a metal after cold working, *Proc. R. Soc. London A143*, 307.

Vasin, V.V. (1973), The stable evaluation of a derivative in the space $C(-\infty, \infty)$, *USSR Comput. Math. Phys. 13*, 16.

Williams, R.O. (1965), The stored energy of copper deformed at 24°C, *Acta Metall. 13*, 163.

Wright, T.W. and H. Ockendon (1992), A model for fully formed shear bands, *J. Mech. Phys. Solids 40*, 1217.

Zehnder, A.T. (1991), A model for the heating due to plastic work, *Mech. Res. Commun. 18*, 23.

Zehnder, A.T. and A.J. Rosakis (1991), On the temperature distribution at the vicinity of dynamically propagating cracks in 4340 steel, *J. Mech. Phys. Solids 39*, 385.

Zehnder, A.T. and A.J. Rosakis (1993), Temperature rise at the tip of dynamically propagating cracks: measurements using high speed infrared detectors, *Experimental Techniques in Fracture*, III, Ch. 5, p. 125.